

Research papers

Sizing of hybrid energy storage through analysis of load profile characteristics: A household case study

E.W. Schaefer^{a,b,*}, G. Hoogsteen^b, J.L. Hurink^b, R.P. van Leeuwen^a^a Saxion University of Applied Sciences, M.H. Tromplaan 17, 7511 JJ Enschede, The Netherlands^b University of Twente, Drienerlolaan 5, 7522 NB Enschede, The Netherlands

ARTICLE INFO

Keywords:

Hybrid energy storage
Storage sizing
Frequency based splitting
Residential

ABSTRACT

Hybrid Energy Storage System (HESS) have the potential to offer better flexibility to a grid than any single energy storage solution. However, sizing a HESS is challenging, as the required capacity, power and ramp rates for a given application are difficult to derive. This paper proposes a method for splitting a given load profile into several storage technology independent sub-profiles, such that each of the sub-profiles leads to its own requirements. This method can be used to gain preliminary insight into HESS requirements before a choice is made for specific storage technologies. To test the method, a household case is investigated using the derived methodology, and storage requirements are found, which can then be used to derive concrete storage technologies for the HESS of the household. Adding a HESS to the household case reduces the maximum import power from the connected grid by approximately 7000 W and the maximum exported power to the connected grid by approximately 1000 W. It is concluded that the method is particularly suitable for data sets with a high granularity and many data points.

1. Introduction

Flexibility is essential in electrical grids with a high penetration of Renewable Energy Systems (RES). Here, flexibility is defined as the capability of a power system to maintain balance between generation and load under uncertainty [1], or in the context of an electric power system, as the ability to vary the performance characteristics of resources to maintain both a balanced as well as an efficient system [2]. More volatility is introduced into electrical grids through decentralized RESs, leading to an increased need for flexibility [2]. This increase can be achieved through control of power demand, alterations of the power production, reinforcement of the electrical grid, power to X,X to power, and Energy Storage Systems (ESS) [3]. Here, ESSs provide valuable flexibility for the electrical grid, by decoupling energy generation and usage in time to match power supply and demand [2] and therefore reduce power imbalances.

In many situations, using a single storage solution is more prevalent than multiple storage solutions. This is mainly due to the cost prohibitive nature of ESSs, and the stage of development of many storage technologies. However, combining multiple complimentary ESSs into a so called Hybrid Energy Storage System (HESS) has potential advantages, specifically in situations where both a quick response is needed as well as a large displacement of energy over time [4]. The main reason for this is that each ESS generally function best at certain time-scales

(for example minute, hour or day–night cycles). This implies that single ESS solutions may be sub-optimal or insufficient in situations where responses on multiple time-scales are required. However, storage size determination of HESSs when accounting for multiple time-scales is challenging.

The energy balances of microgrids across time can be represented by power load profiles. These profiles are the basis for ESS sizing for a microgrid, or for more complicated cases of sizing a HESS where each individual storage component has to be chosen. Furthermore, methods to size individual storage components in a HESS become more manageable when decomposing the balance load profile into multiple sub-profiles. For many applications, a preliminary analysis of storage sizing options is often required at the start of a system design trajectory, in order to have a preliminary indication of how a system can be designed and its feasibility, before more in depth modelling begins. Therefore, an approach for sizing HESSs based on load imbalances is desired which has limited computational time per possible option, wherein the judgement of the designer can be incorporated. This approach should not compete with more in depth approaches such as forecast based approaches (and therefore should not be compared to them), but be used to limit the search space before a more in depth analysis is made. In literature [5] attempts to achieve similar goals, but among other constraints only allows for the sizing of a HESS consisting

* Corresponding author at: Saxion University of Applied Sciences, M.H. Tromplaan 17, 7511 JJ Enschede, The Netherlands.

E-mail address: e.w.schaefer@saxion.nl (E.W. Schaefer).

of two ESSs (see Section 2.2.2 for more on this). There is a need for an overarching technology independent method for finding multiple ESS flexibility requirements for a HESS as a pre-processing step before a more in depth analysis is made. To the best of the authors knowledge this research currently does not exist.

This paper presents a methodology and a tool which give insight into required storage capacities, power rates and ramp rates for a given microgrid scenario, for both a single ESS and a HESS design. No limitations are imposed regarding specific applications or subsets of available storage devices, enabling a broader search space exploration. The methodology aims to give an estimate of the aforementioned values for each individual ESS in a HESS. Furthermore, the computational time of the tool should be kept at a minimum. The derived estimates can be used for further optimization and more detailed considerations, for example when investigating optimal control strategies of microgrids in which storage plays a role. The method is useful in situations where storage technologies have not yet been chosen, where a HESS is considered as a possible solution to handle part of a microgrids power imbalance, and where a large number of options are given and need to be reduced in an efficient way before a more in depth analysis is made. The methodology is demonstrated using a residential use-case.

The contribution of this paper can be summarized follows:

- A novel holistic method for analysing load profiles and deriving a general estimation of required storage capacity, power and ramp rate requirements, for storage devices to be used within a HESS framework.
- A storage independent sizing based approach.
- Investigation into the applicability of the method based on the size of the time granularity.

Section 2 gives an overview of relevant literature, pertaining to load profile analysis, types of storage devices and their characteristics, and sizing of HESSs. Section 3 discusses in depth the multi-step method used to analyse an input load profile and describes the storage model used to ascertain storage sizes. Section 4 presents the scenario used for evaluating the methods, which is a household energy balance for a year, as well as the results of the simulation study. Finally, Section 5 concludes the findings and presents research directions for future investigation.

2. Literature review

In this section, an overview of different energy storage technology categories is given including characteristics of storage, as well as an investigation into (H)ESS sizing techniques, focusing in depth on frequency based load profile decomposition research.

2.1. Storage technologies

Energy storage technologies have been thoroughly investigated and compared in previous research. Explanations of different technologies and comparisons can be found in [6–10]. Storage technologies can be divided into different categories based on storage characteristics. Such categories are useful in simplifying the comparisons based on design criteria. For example, energy storage can be categorized based on the conversion principle and/or the energy carrier in which the energy is stored, as well as the time-scale in which the storage performs optimally. Energy storage characteristics are used to define the categories.

2.1.1. Characteristics

The focus for this research is on storage solutions to which electricity can be exported to and from which electricity can be imported as part of an electrical network. This does not include uni-directional heat storage or other uni-directional conversions. Different characteristics of storage technologies have been identified, from which a selection is given by [7,9] and shown in Table 1.

Table 1

Characteristics of storage devices.

Source: Aggregated from [7,9].

Characteristic
Power rating
Energy rating (Capacity)
Discharge duration at rate power
Storage duration
Daily self-discharge
Response time
Power density
Energy density
Specific energy
Specific power
Round-trip efficiency
Lifetime
Life cycles
Capital cost power
Capital cost energy
Maintenance cost
Maturity level
Environmental impact
Operating temperature

The importance of each characteristic depends on the function the storage needs to fulfil in a specific case. However, characteristics such as power rating, energy rating and capital cost are generally deemed more important than other characteristics. Additionally, only a combinations of characteristics define in which time-scale a storage technology can (optimally) function.

2.1.2. Time-scales

Time-scales are important to categorize storage technologies. They themselves are often closely linked to the function that the storage device can perform. Many overviews in literature compare storage technologies based on two or more characteristics, often using a table or graph, examples of which are given in [11–13]. In fact, because of the multifaceted nature of storage technologies, no single overview can show all characteristics without sacrificing ease of understanding. Fig. 1 from [8] displays an overview of a number of storage technologies. This overview is interesting because it links not only power scale and duration of storage to each technology, but also links categories of functions to the storage. Each circle represents a range within which the storage technology can operate best, the size of the circle showing the maturity of the technologies.

Categories of functions of storage technologies based on time-scales are given in [8]:

- Power Quality and Regulation (\leq one minute). This includes functions such as reactive power control and frequency control.
- Bridging Power (one minute-one hour). This includes emergency power backup and ramping.
- Energy Management ($>$ one hour). This is a broader category including functions such as peak shaving (one-ten hours), transmission curtailment (five-twelve hours), renewable integration and backup (hours-days) and seasonal storage (\geq four months).

These ranges also corroborate the ranges given in [10,14], which are short term, medium term and long term. Based on Fig. 1, no single storage solution functions optimally in all categories.

2.2. HESS sizing

This section investigates the sizing of HESSs. For this ESS indicators are examined, categories of sizing techniques are defined and examples are given in which load profile filtering based sizing techniques are investigated.

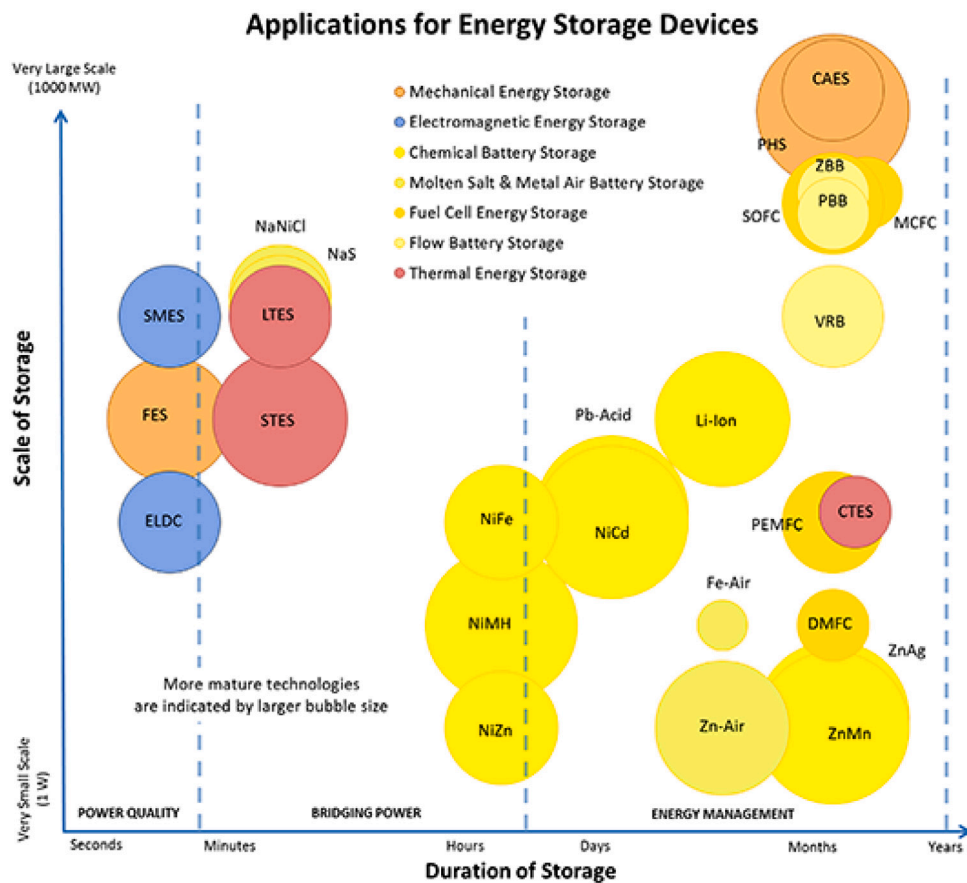


Fig. 1. Applications for energy storage devices [8].

2.2.1. ESS indicators

Performance indicators can be used as optimization criteria to determine the sizing of storage. The criteria can be divided into either the financial or technical category.

According to [15], when using financial indicators there is either a tendency to examine the overall costs and benefits of the system over the operational lifetime of the system or a tendency to try to maximize the market benefit of the inclusion of the ESS in the system. Additionally, the trend is to either maximize the Net Present Value (NPV) or minimize the Levelised Cost of Electricity (LCOE) when optimizing. Using financial indicators has the added benefit of having only a single performance metric, namely currency, which eases comparisons between different solutions.

Yang et al. [15] divides technical indicators into two sets; dynamic characteristics (time periods < one minute) and steady-state characteristics (time periods > one minute). Dynamic characteristics generally encompass the criteria frequency regulation (related more to balance between power supply and demand) and voltage stability (related more to reactive power balance). Steady-state characteristics deal more with criteria such as reliability (for example Loss of Load Expectation or LOLE [16]) and curtailment (for example curtailed power or curtailed accumulated energy). Other potential technical criteria are battery capacity, charge/discharge power rate, battery life cycle, Depth Of Discharge (DOD) and ramp rate (see also Section 2.1.1). These criteria are dependent on the chosen storage technology, and often serve as constraints when choosing a storage solution. As there is no single parameter, often multiple indicators need to be taken as constraints, while aiming to achieve a single objective function.

Finally, both financial and technical aspects can be considered together. Financial indicators often serve to achieve an objective function. However, the technical indicators can either serve as constraints, or

as input for objective functions themselves within a multi-objective optimization process. Considering both financial and technical indicators together has the advantage of potentially forming a clearer model for the given situation. However, weighing indicators properly can be problematic, leading to less accurate sizing choices.

2.2.2. Sizing techniques

Sizing of ESSs has been examined from different perspectives in detail in previous years. In [15] a comprehensive review of sizing techniques for ESSs is given, while [17] does the same for HESSs. An overview of the suitable methods for investigating or optimizing HESS sizing is listed below:

- Analytical methods, in which elements within a power system are varied and performance is analysed. Examples are given in [18, 19].
- Probabilistic/Statistical methods, which mostly use synthetic data generation to analyse a situation based on a small number of performance criteria. Examples are given in [20,21].
- Mathematical optimization based methods, in which optimization problems are expressed as linear, non-linear or mixed-integer programming problems. An example is given in [22].
- Heuristic methods, in which algorithms (often local search algorithm such as Genetic Algorithms (GA)) can be used to solve an optimization problem. Examples are given in [23,24].
- Ragone method, in which a Ragone plot is used to compare relevant indicators of ESSs. An example is given in [25].
- Pinch analysis method, which is a methodology specifically tailored for heat exchange networks. Examples are given in [26, 27].

Table 2
Overview of previous research using filtering method.

	[28]	[18]	[29]	[30]
Method	Analytical	Analytical	Hybrid	Analytical
Off grid	No	No	Yes	Yes
Other flexibility	Yes, main grid	Yes, main grid	No	Yes, generator
Load profile sample frequency(s)	900	1	1	60
Number of ESSs	2 (note, no specific device chosen)	2 (Supercapacitor and Fuel cell)	3 (Lead-acid, Li-ion, Supercapacitor)	2 (Battery and Supercapacitor)
Life cycle	No	No	Yes	Yes
Losses	No	Yes	No	Yes
DOD	Yes	No	No	Yes
Power rate	Yes	Yes	Yes	Yes
Ramp rate	Yes	Yes	No	No
Cost	No	No	Yes	Yes
Cut-off frequencies	Manual	Manual	Algorithm	Algorithm

The aforementioned methods can also be used in combinations. Additionally, in [4] it is stated that HESS sizing methods may differ from methods for ESS sizing. Some methods for ESS sizing may prove impractical or impossible to be used for HESS sizing, as the fact that multiple combinations of possible solutions exists greatly increases the design space. In addition there is more of a focus on total cost and system reliability in HESS sizing methods.

One further investigation is noteworthy, found in [5], specifically because it is the only method found that attempts to investigate HESSs without first choosing specific technologies. It presents a method which sizes two separate ESSs for a single HESS system, where one ESS is more responsible for power and one ESS is more responsible for energy. This has the advantage of more strictly sizing the ESS taking into account that the ESSs not needlessly charge each other. In addition, the fact that the analysis is not technology dependent has inherent advantages (see also Section 2.2.3). However, in [5] the analysis is restricted to only two ESSs. Furthermore other flexibility assets cannot be accounted for directly in the analysis (for example a grid connection), but only in pre-analysis. Finally, ramp rates are not accounted for, which means an incomplete image of flexibility requirements from each ESS is presented.

2.2.3. Frequency based load profile splitting for HESS sizing

This section investigates in depth the current usage of frequency based load profile splitting in HESS sizing research. Frequency based load profile splitting is a technique used for sizing multiple storage devices in a HESS by analysing a power load profile to be handled by a HESS and splitting it into multiple sub-profiles, each to be handles by a single storage solution. This technique is generally used as a part of a more analytical type of approach. Of the available research in this area, four specific publications [18,28–30] illustrate points relevant for this paper. In mentioned papers a combination of DFTs (Discrete Fourier Transform) and discrete filtering is used. An overview of the content of these papers is given in Table 2, which includes technical and financial indicators. A more comprehensive overview of recent research in this area, which is not limited to frequency based load profile splitting, is given in [17].

All mentioned publications use DFTs and IDFTs (Inverse Discrete Fourier Transform) in order to analyse the band of the given load profile. Additionally discrete filtering is used in order to split the load profiles into sub-profiles, by using low-pass, band-pass or high-pass filters, or combinations of the three. Each publication also refers specifically to a situation for which a HESS size should be chosen, and tailors the method to size for that situation.

Zhao et al. [28] present a wind farm scenario in which hybrid storage should be used to smooth out the imbalance, with imbalance defined as the difference between the generation and the consumption profile. The load profile is divided into four separate sub-profiles, each with a corresponding time interval:

- Very Short Term (one half-one hour)

- Short Term (one-five hours)
- Intra-day (six-24 h)
- Outer-day (24+ h)

This is a slight deviation from the time-scales mentioned in Section 2.1.1. Due to the sample frequency of the data, no events shorter than 900s (0.25 h) are taken into account. This also implies that potential storage devices matched to this band may not be properly suited to events smaller than 15 min. In the paper, the storage sizing approach is not discussed, and no specific storage elements are chosen, meaning no technology specific indicators are investigated, although a maximum DOD of 90% is chosen. Two scenarios are investigated, one in which all four sub-profiles are assigned to a storage, and one in which the two sub-profiles with the highest frequency bandwidths are assigned to a storage. This is in order to reduce the storage required and examine a potentially more feasible solution.

San Martín et al. [18] investigate the integration of a fuel cell and a supercapacitor for a microgrid containing PV, wind as well as simulated household loads. Charge and discharge losses are modelled, and the storage degree of coverage, in this context defined as how often the system can function using only storage without a grid connection, is examined in relation to energy capacity for a hydrogen system. The supercapacitor cut-off frequency is examined in relation to the required storage capacity. What is interesting here is that although a frequency filtering approach has been used, i.e. a high pass filter is used to separate the profile into sub-profiles, a solution was found manually which compromises between the size of the supercapacitor, the reduction in variability covered by the hydrogen system, as well as the power exchange with the main grid.

Wen et al. [29] detail a more specific situation than the other papers by investigating a HESS for a ship powered by PV and diesel. The main goal is to smooth out the imbalance profile, which is more erratic than a general PV profile due to the movement of the ship at sea. Three specific storage technologies have been chosen, lead-acid, li-ion and supercapacitor. PSO (Particle Swarm Optimization), in combination with DFT has been used to iteratively investigate which two cut-off frequencies are optimal from a cost perspective. This method uses technical indicators as constraints, and cost as the main indicator for the optimization objective.

Finally, Liu et al. [30] investigate a situation similar to [28], in which a network has a high penetration of PV, although in this case the network is off grid, but does include a generator for extra flexibility. The main goal of the HESS is to smooth out the imbalance profile, which here is defined as the difference between the predicted wind generated power and the actual wind generated power. Again, DFT is used to analyse the load profile. Here, a high cut-off frequency is first chosen iteratively using a Power Spectral Density (PSD) based method, in order to define which frequency band of the original load profile is to be handled by the generator. Then, the low cut-off frequency (between the battery band and the supercapacitor band) is iteratively chosen, while minimizing costs. Indicators such as SoC and charge/discharge

losses have been modelled in a more general way, i.e. not based on the specific constraints of the discussed storage technologies. Cycle life of the storage device has been calculated based on the specific storage technology.

In the mentioned researches, there is a risk that splitting the profiles while keeping certain storage technologies in mind introduces a certain bias, as this way limits the search space already to one or two solutions. When specific technologies are added early in the process, technical indicators are introduced as constraints, making any conclusions drawn specific to the technology introduced as opposed to a set of possible storage devices. Furthermore, due to the varying goals, specific situations and indicators used, no specific HESS sizing method seems to be used, other than the general notion of splitting up load profiles into sub-profiles based on the fact that storage technologies function (best) at a specific time-scales.

Given the above considerations, it is of interest to develop a methodology for finding HESS storage requirements for a given situation based only on the load profile, without making a specific choice of storage technologies beforehand. This will allow for both an unbiased analysis as well as the consideration of different storage technologies at a later phase in the design trajectory.

3. Methods

Selecting storage sizes for individual ESSs in a HESS is challenging. The main problem is to assign which ESS in a HESS framework is responsible for which time-scale behaviour, and to choose the sizing requirements of those ESSs accordingly. Gaining insight into time-scale behaviour can be achieved through the analysis of an imbalance load profile. However, there is no practical way to inherently link the behaviour of a single load profile to the set of storage devices. Frequency filtering provides a solution by splitting up the load profile into multiple sub-profiles and subsequently linking each sub-profile to an ESS. This paper proposes a method to split an imbalance load profile into multiple sub-profiles, each representing a time-scale relevant within the original load profile, and then use these sub-profiles when dimensioning storage devices. As discussed in Section 2, most research starts analysing having already chosen specific storage technologies to be used. This method proposes to start with sizing instead, thereby remaining storage technology independent, and not limiting the search space.

The proposed process, detailed in the following sections, is divided into three steps. Step one is pre-processing, where the imbalance load profile of the considered microgrid is created. Step two contains the main processing and makes a preliminary selection of filter cut-off frequencies and creates the resulting sub-profiles. Step three is post-processing, where the created sub-profiles are analysed for sizing flexibility requirements, and a decision is made to either iterate with updated cut-off frequencies and create new sub-profiles or use one or more of the derived sub-profile to dimension storage for the time-scale of the selected sub-profiles.

3.1. Pre-processing

An imbalance profile is required for the creation and dimensioning of a HESS. However, it is not always clear in a practical setting how the profile is derived. In the following two often occurring situations are observed.

Option one considers the entire imbalance of a given profile for a specific (micro)grid to be the responsibility of the HESS to solve. In other words, no power exchange is required from a connected grid or through other means to achieve power balance. The load imbalance P_{imb} for this option is now just the sum of the power demand by the load P_{dem} and the production P_{prod} , all at moment t as shown in (1). In

this paper we use the convention that positive power and energy are load and negative are production, unless stated otherwise.

$$P_{imb}(t) = P_{dem}(t) + P_{prod}(t) \quad (1)$$

Option two considers that a part of the flexibility can be handled through a grid connection, where a maximum power exchange is accounted for. This situation is expressed in (2), where $P_{grid,max}$ defines the maximum power exchange with the grid, $P_{imb,o}$ is the original grid imbalance and $P_{imb,s}$ is the new grid imbalance to be handled by storage. Here, the power exchange is considered to be symmetrical, however separate grid import and export values can be chosen if desired. Note that $P_{grid,max}$ is considered to be time dependent, although in many situations a single value may be given for the entire time series.

$$\begin{aligned} P_{imb,s}(t) &= P_{dem}(t) + P_{prod}(t) + P_{grid,max}(t) \text{ if } P_{imb,o}(t) < -P_{grid,max}(t) \\ P_{imb,s}(t) &= 0 \text{ if } -P_{grid,max}(t) \leq P_{dem}(t) + P_{prod}(t) \leq P_{grid,max}(t) \\ P_{imb,s}(t) &= P_{dem}(t) + P_{prod}(t) - P_{grid,max}(t) \text{ if } P_{imb,o}(t) > P_{grid,max}(t) \end{aligned} \quad (2)$$

In principle, any power load profile $P_{imb,o}$ can be used from use cases where one or more storage devices are required. Examples are situations such as neighbourhoods, industrial parks and off-grid microgrids. Additionally, any time step granularity of the load profile can be used. However, the choice of this granularity has consequences for the usefulness of derived sub-profiles in ascertaining storage requirements (see Section 4). It is preferable to have a time step granularity as small as possible (sub-minute), as this allows for the most precise view of the imbalance.

3.2. Processing

This subsection details the processing method for the created imbalance profile, which is to be handled by storage devices. The processing step details the decomposition of a single imbalance load profile into multiple sub-profiles through the use of discrete signal filters, discussed in Section 2. First, the filter cut-off frequencies must be selected. Next, the resulting sub-profiles must be created by splitting the original profile into multiple sub-profiles.

As stated in Section 2, storage devices are designed to work (best) at particular time scales, specific to that type of storage. It is intuitive to therefore create time-scale based sub-profiles derived from the original imbalance profile and centred around that time-scales power fluctuations.

3.2.1. Selecting cut-off frequencies

Selecting cut-off frequencies for filtering can be tricky. As discussed in Section 2, this can be done either manually by the user or through the use of algorithms. This method proposes choosing the frequencies through one of two options, both of which are considered to be manual, as they rely on the insight of the designer.

Option one forgoes any further analysis of the input load profile itself, and focuses on the time-scales which represent behaviour that (groups of) storage can enable. A guideline here can be Fig. 1, but also other divisions of time-scales can be used that are suitable for the case under investigation. This option has the advantage of choosing a starting point that is close to potential time-scales of storage solutions, but has the disadvantage of not taking the structure of the imbalance load profile itself into account, possibly increasing the need to iterate after post-processing and re-select cut-off frequencies.

Option two is more of a brute force approach, which examines a wide variety of cut-off frequencies, a so called sub-profile band analysis approach. Here, a number of suitable low and high cut-off frequencies are chosen which are within the bounds of the given data. Then, a large number of test sub-profiles are created, one for each unique combination of low and high cut-off frequencies, or bands. Subsequently, each test sub-profile is analysed and its flexibility characteristics are retrieved, specifically capacity, maximum power, minimum

power, maximum ramp rate and minimum ramp rate (see Section 3.3.1 for more on this). Finally, a heat map is created for each flexibility characteristic for further analysis. The set of heat maps created then act as guidelines for the designer to choose a set of cut-off frequencies for creation of the sub-profiles. Heat maps are useful here as they give the relationship between different values in a clear context, which allows for greater ease of band selection. The advantage here is that the designer gains insight into a number of possible combinations of sub-profiles, while a disadvantage is that this approach increases complexity as each flexibility characteristic must be evaluated individually while taking the others into account.

It is noteworthy that the time step size of the original load profile is a constraint which must be accounted for when choosing cut-off frequencies. The Nyquist frequency is twice the frequency of the original signal and ensures the filtered signal is free of aliasing [31], meaning that filtered profiles are free of distortions. Sub-profiles must be avoided where a cut-off frequency is higher than the Nyquist frequency of the original load profile. Additionally, it is not recommended to create a profile where the cut-off frequency is lower than $1/Samples$, where $Samples$ represents the total number of samples in the data set, as time-scale behaviour will not be distinguishable.

3.2.2. Creating sub-profiles

The creation of sub-profiles is done in an iterative manner. The flow chart Fig. 2 illustrates the splitting of a load profile into sub-profiles. Each time the given load profile is filtered using a cut-off frequency, a corresponding time-scale sub-profile is created. Here, a low-pass filter [32] is used, which filters out higher frequencies than the cut-off frequency, and allows lower frequencies to pass. The remaining unfiltered profile can then be filtered by the next low pass filter with a higher cut-off frequency, until the entire set of cut-off frequencies has been filtered. In principle, high-pass filters or band-pass filters could also be used, although the resulting sub-profiles may vary due to filter roll-off frequencies. A low-pass filter has the added potential advantage of creating neater lower frequency sub-profiles, which could be useful when linking these sub-profiles to specific slower working storage technologies, in which more predictable behaviour is desirable. Additionally, any rest behaviour as a result of adhering to the Nyquist frequency when filtering at the highest possible frequencies should be handled by a storage device which works best at these time-scales, and not added to the lower frequency filtered bands. The order of the filter is chosen to be 2nd order, as it has a sharper roll-off than a 1st order filter. A sharper roll-off leads to a more clear cut filtering of bands, which is desirable.

The relationship between the original profile and x number of sub-profiles at moment t is given in (3), where P_t is the original load at time t , and P_t^n is the filtered load at time t for the n th sub-profile.

$$P_t = \sum_{n=1}^x P_t^n \quad (3)$$

3.3. Post-processing analysis

This sub-section details the post-processing phase, including determination of the storage requirements as well as the overall evaluation of the profiles.

3.3.1. Storage requirements

Flexibility of systems can be characterized by several metrics and indicators, dependent on a specific situation [33] or as part of a more generalized framework [34]. Useful flexibility metrics for analysis and assessment of power systems are power, energy and ramp-rate [35]. These metrics can also be taken as specification of storage device requirements, and can be derived using the sub-profiles from the previous section.

Power rates per sub-profile can be found by investigating the maximum and minimum power values in that sub-profile. As the power

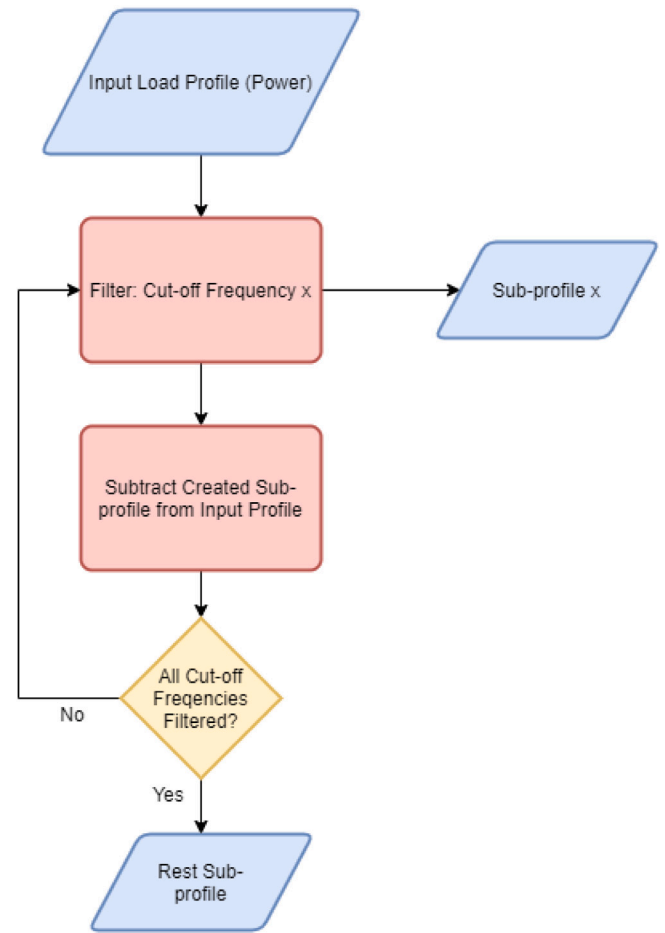


Fig. 2. Flowchart for splitting a load profile into multiple sub-profiles.

profiles can have both positive and negative values (to represent both positive and negative imbalances), both maximum and minimum values should be derived.

In order to find the ramp rate (R_r), (4) is used, where t is the current moment, $t - 1$ is the previous moment, and T_s is the sample time in seconds.

$$R_r = \frac{P_{imb}(t) - P_{imb}(t-1)}{T_s} \quad (4)$$

To find the required storage capacity for a sub-profile, a storage charge profile must be created for that sub-profile. This storage charge profile shows the relative charge contained within the storage at any given moment, and can be both positive and negative, see (5), where E_t is the energy stored at a given moment in Wh, P_{imb} is the power imbalance. Unless otherwise stated, all energy values in this paper are given in Wh.

$$E_t(t) = E_t(t-1) - P_{imb}(t) \cdot \frac{T_s}{3600} \quad (5)$$

In order to get the total required storage capacity, E_{cap} , the maximum value of the storage capacity profile $E_{t,max}$ and the minimum value of the storage capacity profile $E_{t,min}$ are used, see (6).

$$E_{cap} = E_{t,max} - E_{t,min} \quad (6)$$

Note that here no storage losses, for example conversion losses, are accounted for. This is purposeful as the goal is to derive a generic indication of the storage requirements. Taking losses and other storage technology specific factors such as Depth of Discharge (DOD) into account would limit the search space, which is not desired at this stage.

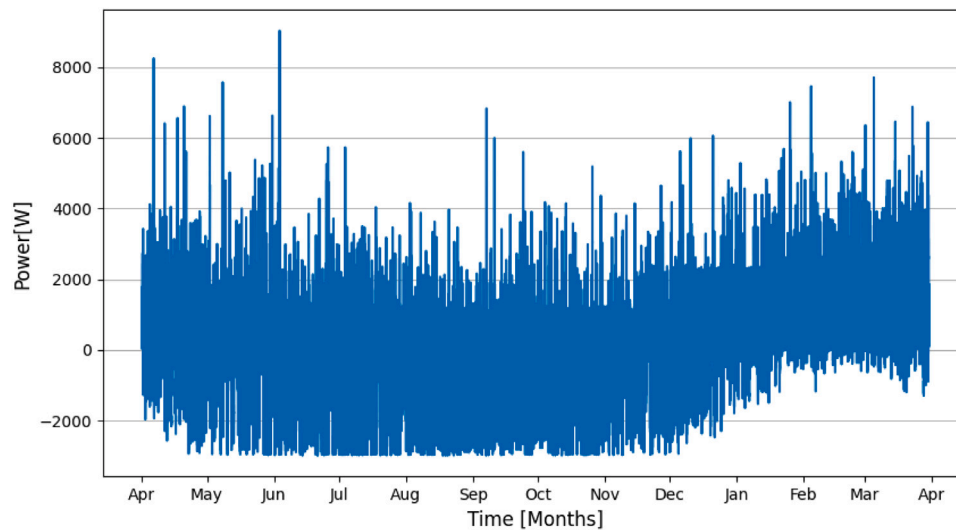


Fig. 3. Load profile data, 1 year.

Table 3

Load profile metadata.

Name	Value
Sample frequency	0.1 Hz (10 s)
Samples	3 144 734
Total energy	-625 975 Wh
Minimum power	-2980 W
Maximum power	9030 W
Minimum ramp rate	-517 W/s
Maximum ramp rate	523 W/s

A similar reasoning is used for battery control. In order to ascertain the storage sizing, the control is chosen to be greedy. Here, when there is an excess of energy available in a sub-profile, E_{stor} is increased by this excess, and when there is a deficit of energy available E_{stor} is decreased by this deficit. Taking specific control strategies into account would also limit the search space, as control strategies can be based on the aggregated flexibility in a system (i.e., the sum of the storage devices, as well as other available flexible devices) in a multitude of ways. Also, if prediction is part of the control strategy, this introduces an extra level of complication which is not desired in a preliminary investigation. Note, over-dimensioning may be a result of trying to cope with prediction errors.

3.3.2. Evaluation of profiles

Based on the created sub-profiles, a choice can be made to accept the sub-profiles as they are or to iterate. Here, iteration means either returning to the pre-processing step and altering the input imbalance, or returning to the processing step, whereby cut-off frequencies are altered and new sub-profiles are created. Furthermore, if the achieved set of sub-profiles is considered to be acceptable, a choice can be made of which sub-profiles can function as storage and which should not be considered storage. This means that, although the intention in the pre-processing phase is to cover the entire imbalance through storage devices and steps were taken to account for connected grid flexibility, it may prove useful to re-add sub-profiles which are not suitable for storage to any remaining flexibility imbalance which are, for example, handled by a grid connection.

Guidelines for deciding which sub-profiles are suitable to be handled by storage are case and goal specific and are likely linked to required technical functions and/or financial incentives. However, such guidelines are not within the scope of this method. As an example, if five sub-profiles have been created, three may be handled by storage and two could be considered to be the remaining imbalance and

not handled by storage. This consideration is based on the available financial capital and the flexibility available through other means, for example through a connection to a larger grid or backup generators.

4. Evaluation

In this section, an evaluation test-case and simulation results are presented. The test-case concerns a household where storage should be implemented. The main goal is to investigate the generic storage requirements per sub-profile for the household using the method presented in Section 3. An additional goal is to examine the impact of using the proposed method with different input load profile sample frequencies.

We have implemented the method presented in Section 3 into a tool in Python, the so called Load Profile Analysis Tool (LPAT). LPAT is free to use for non-commercial ends (NC-BY licence), and available at [36]. This tool takes a load profile as input and performs the splitting into sub-profiles as well as the flexibility characteristics analysis of the sub-profiles based on set parameters. Furthermore, the computational time of the tool is evaluated.

4.1. Model

The load profile data used for the model are taken from a real world measured energy balance of a household, see Fig. 3. The household is located in the Netherlands, and is all electric (does not use natural gas and uses a wood stove for heating). It has an electric boiler which is used for heating water, and an induction cooking stove. Furthermore the house also produces energy with solar panels.

The data considered in this evaluation was collected between February 2018–January 2019, with the exception of May, where data from 2019 was used instead. No large differences in demand load (i.e. new appliances) are known to have occurred during this time, making May 2019 suitable to use. The data was collected using a monitoring system connected to the smart meter located at the point of connection to the grid of the household, with a sample frequency is 0.1 Hz. Of the remaining months, the majority of the data in that year was measured, with <0.005% missing. The missing data is spread out over the year, and not concentrated in specific moments. For larger gaps (>4 h), missing data is replaced with a zero value. For the remaining gaps, no data was added. After making the alteration to the data set, we consider the data to be a good representation of the household case.

Table 3 displays the general information regarding the load profile. Note that the total energy of the year is negative (-626 kWh), meaning that the household produces more energy over a year than it consumes.

Table 4
Sub-profile ranges.

Name	Frequency (Hz)	Time
Profile 1(P^{dy}) Energy Management Long	$P^{dy} \leq \frac{1}{86400}$	$P^{dy} \geq 1 \text{ d}$
Profile 2(P^{hr}) Energy Management Short	$\frac{1}{86400} > P^{hr} \geq \frac{1}{3600}$	$1 \text{ h} \leq P^{hr} < 1 \text{ d}$
Profile 3(P^{mn}) Bridging power	$\frac{1}{3600} > P^{mn} \geq \frac{1}{60}$	$1 \text{ min} \leq P^{mn} < 1 \text{ h}$
Profile 4(P^{rs}) power Quality and Regulation	$P^{dy} > \frac{1}{60}$	$P^{dy} < 1 \text{ min}$

Table 5
1 year sub-profile data, 10 s sample frequency.

	Capacity (Wh)	Min power (W)	Max power (W)	Min R rate (W/s)	Max R rate (W/s)
Original profile	1904028.4	-2980.0	9030.0	-5.17E+02	5.23E+02
P^{dy}	1886593.4	-797.2	762.5	-5.91E-04	5.47E-04
P^{hr}	31386.7	-1501.7	1048.3	-8.39E-02	8.47E-02
P^{mn}	7177.4	-2531.5	6305.8	-9.23E+00	1.04E+01
P^{rs}	190.8	-3177.6	5604.8	-5.11E+02	5.27E+02

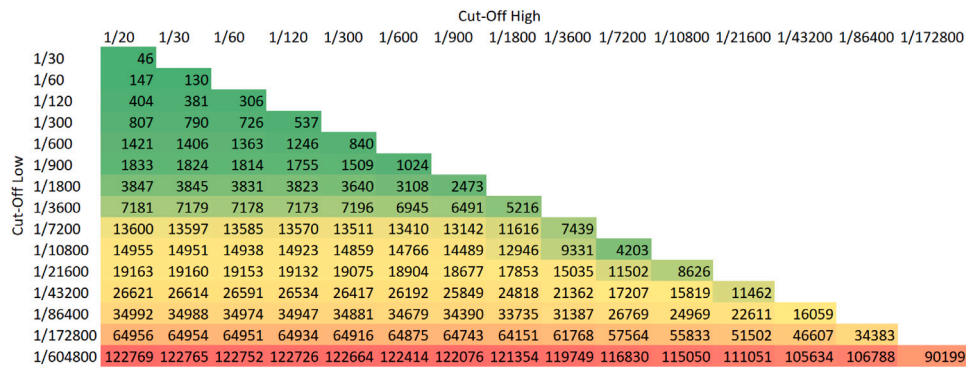


Fig. 4. Capacity heat map. (For interpretation of the references to color in this figure legend, the reader is referred to the web version of this article.)

Based on this data, a 2nd data-set was created, re-sampled to a sample frequency of 900 s (15 min) average values, in order to explore the effects of data granularity on the results derived using the proposed method.

4.2. Pre-processing

The household data represents the power exchange of the household with the main grid. This is the imbalance that must be dealt with from the electrical circuit outside the household, and is the sum of the energy production and energy demand at any given moment. This imbalance profile is assumed to be completely handled by storage, and therefore this original imbalance profile has to be split into sub-profiles in the processing step.

4.3. Processing

During the processing, the cut-off frequencies are selected and based on this selection the imbalance load profile is split into several sub-profiles.

4.3.1. Selecting cut-off frequencies

The cut-off frequencies chosen are $\frac{1}{86400}$ Hz (corresponding to 1 day), $\frac{1}{3600}$ Hz (corresponding to 1 h) and $\frac{1}{60}$ (corresponding to 1 min). The ranges of the created sub-profiles are given in Table 4. These sub-profiles were chosen because they are in line with the storage technologies ranges given in Fig. 1, and deemed suitable for this particular case.

As mentioned in Section 3, it is possible to examine an imbalance load profile in more depth first before making a choice of cut-off frequencies, which can make the resulting sub-profiles better attuned to

the specific imbalance load profile input. This so called band analysis approach is carried out for the purposes of this paper. A set of heat maps was created for several possible sub-profiles using sub-profile band analysis. The sub-profile band analysis uses a number of cut-off frequencies in order to investigate capacity in Wh (Fig. 4), maximum and minimum power in W (Figs. 5 and 6) and maximum and minimum ramp rate in W/s (Figs. 7 and 8) per band investigated, in order to gain an overview of the set of possible bands. The cut-off frequencies are shown in the figures, given in Hz, with the high cut-off frequency shown horizontally, and the low cut-off frequency shown vertically. Each cell shown that bands specifically calculated capacity, power or ramp rate value. The cut-off frequencies were chosen based on the sample frequency and data size. Based on the Nyquist frequency, $\frac{1}{20}$ Hz is the highest possible frequency. As the data is for one year, $\frac{1}{604800}$ Hz (a week) is a good lower frequency limit. The intermediate frequencies were not chosen regularly, as the computational time required to carry this out would be large. However, representative frequencies were chosen which give a good indication of different ranges.

It is clear by the colours and values in Fig. 4 that the low cut-off frequency value is leading when determining capacity. In this case, the lower the low cut-off frequency, the larger the required capacity. Figs. 5 and 6 show that both the low and the high cut-off frequency effect the maximum and minimum power requirements, where a larger difference between both values means a larger power is required. Finally, Figs. 7 and 8 show that the ramp rate is mainly influenced by the high cut-off frequency, with a lower value requiring a higher ramp rate. This conforms to expectations, as it is intuitive that the higher frequency bands contain the most drastic and quick changes, and therefore the highest ramp rates.

Additionally, the heat maps can be used to choose cut-off frequencies for the sub-profiles if so desired. This is based on the specific requirements of a use case. For example, a decision can be made by

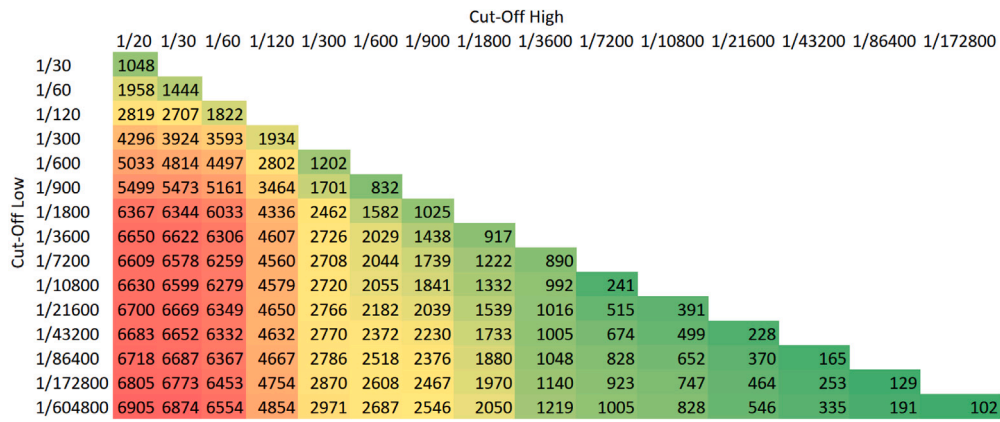


Fig. 5. Maximum power heat map. (For interpretation of the references to color in this figure legend, the reader is referred to the web version of this article.)

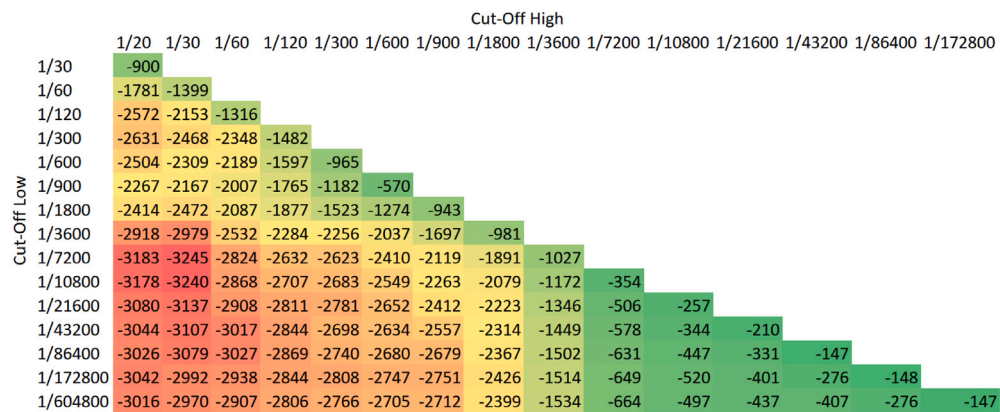


Fig. 6. Minimum power heat map. (For interpretation of the references to color in this figure legend, the reader is referred to the web version of this article.)

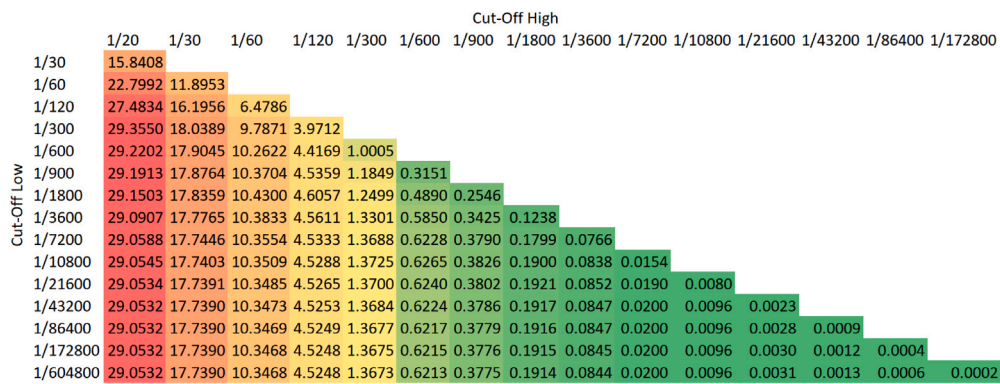


Fig. 7. Maximum ramp rate heat map. (For interpretation of the references to color in this figure legend, the reader is referred to the web version of this article.)

a designer to design a HESS with three ESSs to handle the imbalance of a microgrid. No storage devices have been selected yet, but it is intuitive to have each sub-profile specialize in one specific flexibility characteristic. Storage one is selected to focus on ramp rate. The heat maps show that in the band 1/120 to 1/20 Hz, ramp rate is relatively high (red), capacity is relatively low (green), but power is in the middle (yellow) relative to the other power values. A bandwidth with a lower high cut-off can be chosen, for example 1/60 Hz, but this would lead to a relatively lower ramp rate (orange). The choice is made in this case to keep the band at 1/120-1/20 Hz. The process is then repeated for the other two storage devices, one specializing in power and one specializing in capacity.

As stated at the beginning of the section, for this paper cut-off frequencies are selected corresponding to the values in Table 5.

4.3.2. Creating sub-profiles

The sub-profiles created from the 10 s load profile data are shown in Fig. 9. Each graph represents a sub-profile achieved using the settings detailed in Table 4, as well as the original load profile. The graphs increase in volatility from top to bottom, reflecting the increase in the frequency.

For clarity, P^{hr} , P^{mn} and P^{rs} have been enlarged to show the behaviour over shorter time spans. Fig. 10 shows a zoomed in graph of sub-profile P^{hr} for approximately two days. Here, the recurring behaviour can be seen, where a wave period has a one day period. Fig. 11 zooms in on P^{mn} to show approximately six hours, where two clear wave periods can be seen, or one period approximately every three hours. Finally, Fig. 12 zooms in on P^{rs} for approximately an hour. Here, multiple shorter wave periods can be seen. There is less

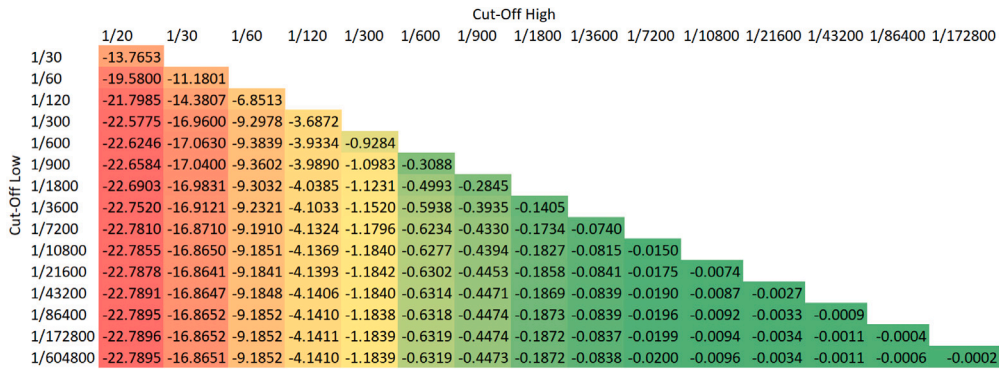


Fig. 8. Minimum ramp rate heat map. (For interpretation of the references to color in this figure legend, the reader is referred to the web version of this article.)

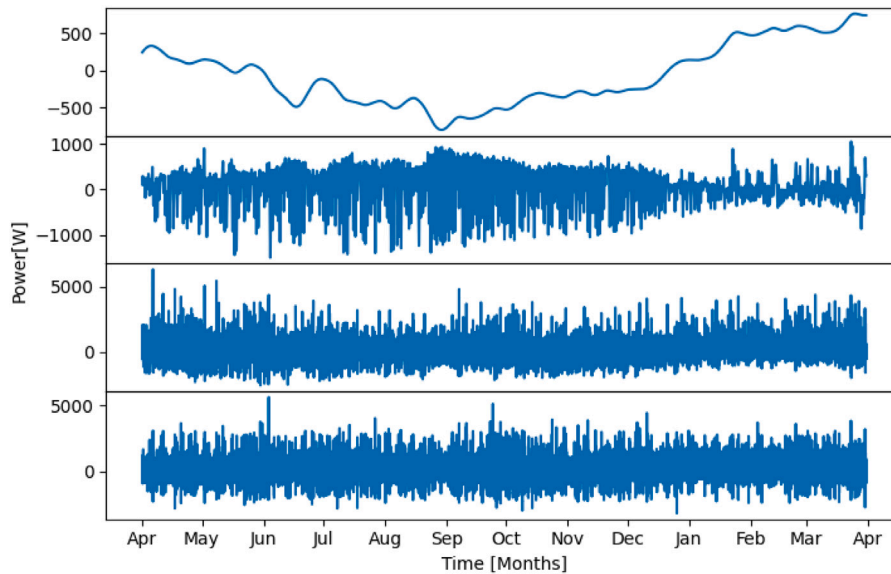


Fig. 9. Sub-profiles one year, P^{dy} (top), P^{hr} (2nd from top), P^{mn} (2nd from bottom) and P^{cs} (bottom).

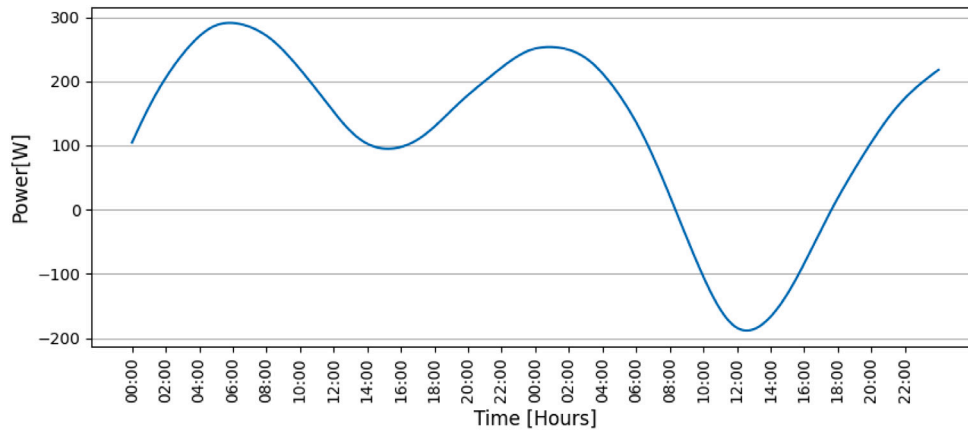


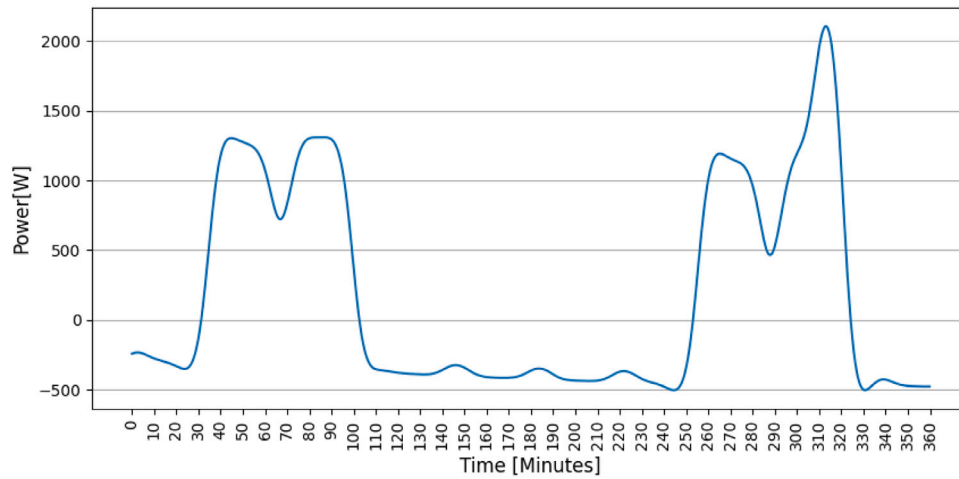
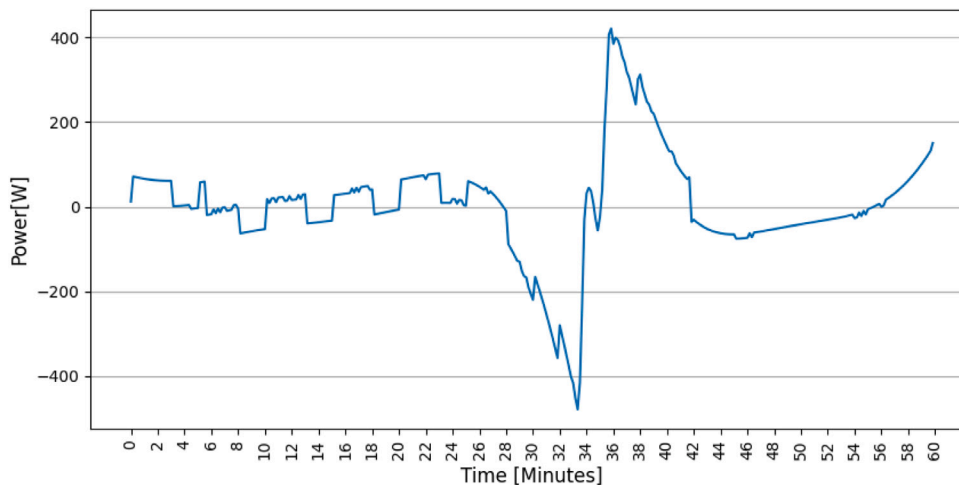
Fig. 10. P^{hr} sub-profile, two days.

of a period trend visible here due to the frequencies in the band being the remainder of the original signal.

4.4. Post-processing

In Table 5 an overview of the characteristics of the achieved sub-profiles as well as the of original profile is given. Also, the required

capacity of a storage device service these profiles is given. A few points are noteworthy. First, the required capacity decreases as the frequencies within each sub-profiles band becomes faster. Second, the minimum and maximum power decreases as a general trend, as the frequencies within each sub-profiles band becomes slower. This leads to the conclusion that the higher power components of the load profile take place at shorter time-scales for this case. Here, the maximum

Fig. 11. P^{mn} sub-profile, six hours.Fig. 12. P^{rs} sub-profile, one hour.

power between P^{mn} and P^{rs} is an exception to this, as P^{mn} requires more power than P^{rs} . Next, both the minimum and maximum ramp rates increase as the frequencies within each sub-profiles band becomes faster. This is to be expected, as the behaviour in these higher frequency time-scales is faster. Lastly, the required characteristics for the original profile and the profile P^{dy} capacities do not differ so much, however the power differs greatly, specifically the maximum power.

Both the decreasing capacity and the increasing power requirements for increasing frequency ranges are in line with what is required by storage devices in respect to time-scales. As demonstrated in Fig. 1, storage devices generally trade power for capacity. In the case that storage devices should serve (some) sub-profiles, it is probable that storage technologies exist which meet the sub-profile requirements. This indicates that the proposed method may have value as a preliminary investigation tool.

Storage charge profiles are also constructed using the approach outlined in Section 3 showing a relative charge at any given moment for the sub-profiles. These correspond to the profiles shown in Fig. 9. These profiles are given in Fig. 13. Two observations can be made. First, the original profile and the profile P^{dy} storage profiles look very similar, which is in line with the minimum difference in storage capacities. Second, each profile shows how a cycle can behave. The lower frequency sub-profiles have longer cycles (fully charging and fully discharging once is a cycle), and the higher frequency sub-profiles shorter cycles.

Considering the above, it seems not to be practical for this use case to use storage to handle sub-profiles P^{dy} and $P^{hr,s}$ as the required storage capacity is too large and seasonal storage is not practical at household level. An iteration, where grid constraints are taken into account in pre-processing or other cut-off frequencies are chosen, is possible. However, the choice has been made here not to iterate, but to assume both P^{dy} and P^{hr} can be handled by means other than storage. Additionally, it is assumed that sub-profiles P^{mn} and P^{rs} are suitable to be considered storage profiles. Therefore, it is interesting to see what the effect is of removing these two profiles from the original imbalance by subtracting load P^{mn} and P^{rs} from the original load profile. In other words, what is the effect on the original grid imbalance of adding the P^{mn} and P^{rs} based HESS flexibility to the microgrid?

Fig. 14 shows this improved profile, which has a much lower maximum power requirement, and a lower minimum power requirement. It is interesting to note that the demand of the microgrid seems to be contained more in P^{mn} and P^{rs} , as much of the positive part of the improved profile appears flatter. The production appears to have a higher percentage of power than the demand covered by the other sub-profiles, as the negative part of the improved profile appears less flat. This means that the production behaviour has a slower time-scale component.

Fig. 15 is a load duration curve taken from the original and improved load profiles given in Fig. 14. What is clear here is that the improved profile when storage is added to the household does not

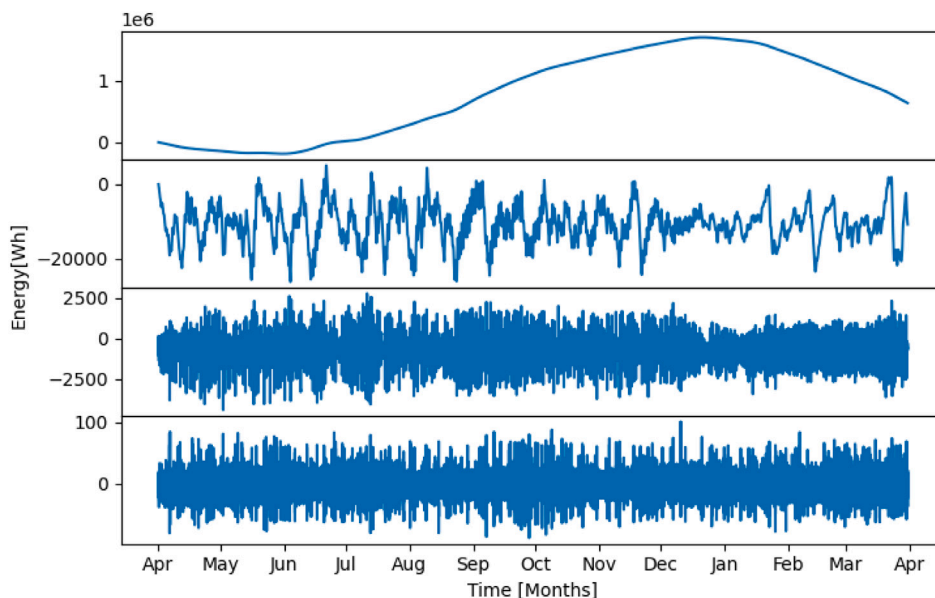


Fig. 13. Storage profiles one year, P^{dy} (top), P^{hr} (2nd from top), P^{mn} (2nd from bottom and P^{rs} (bottom).

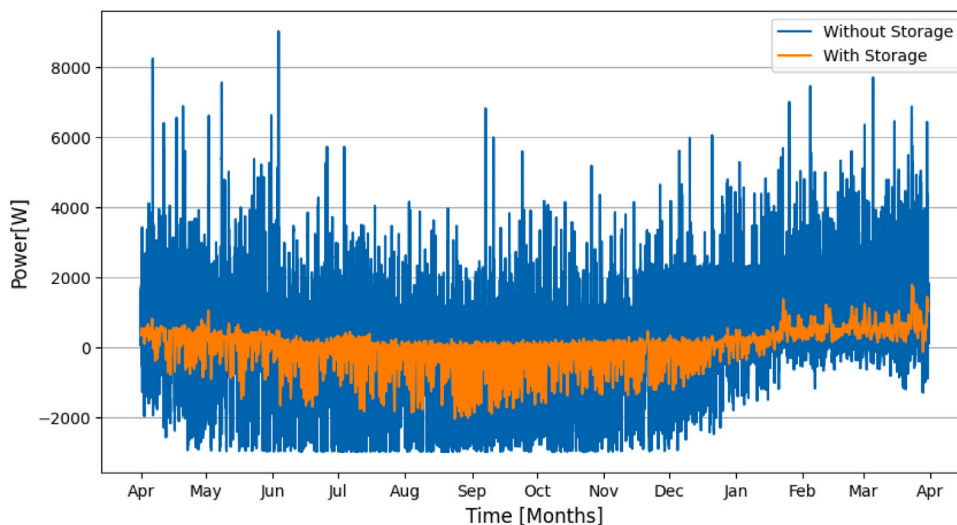


Fig. 14. Improved energy balance, one year.

often have an value of 1000 W or higher. This appears approximately $\frac{1}{30}$ th of the year, in comparison to the original profile where this occurs approximately $\frac{1}{7}$ th of the year. In addition, the maximum power (imported from the grid) of the improved profile is approximately 2000 W in contrast to the original profile where the maximum power value is approximately 9000 W, which is a marked improvement. For minimum power (exported to the grid), the differences are less pronounced, where the improved profile is approximately 2000 W in comparison to the original profile which is approximately 3000 W.

4.5. Downscaled data

This section investigates the influence of the frequency of the input load profile. For this, a new input load profile data set was created from the 10 s data set, by averaging 90 consecutive intervals, leading to 15 min (or 900 s) intervals. The downsampled year load profile and the corresponding sub-profiles are shown in Fig. 16. There is one profile fewer than in Section 4.3.2, due to the sample frequency being lower than the cut-off of P^{mn} as in Table 4. This means that P^{mn} is not created and P^{rs} covers the remaining band above a cut-off frequency of $\frac{1}{3600}$.

Table 6

Comparison of storage sizes one year for original (10 s) and downsampled (900 s) data set.

Profile name	Capacity 900 s (Wh)	Capacity 10 s (Wh)
P^{dy}	240 100.3	1 886 593.4
P^{hr}	1 719 423.6	31 386.7
P^{mn}	–	7177.4
P^{rs}	94 757.3	190.8

It is immediately evident, in comparison with Fig. 9, that almost all of the fluctuating behaviour is now in P^{rs} . In addition, as shown in Table 6, the storage size for P^{rs} is higher than in the 10 s analysis. If the storage capacity requirements of P^{mn} and P^{rs} from the original 10 s data are combined, the 900 s data required storage capacity is more than twelve times larger. It is also uncertain what is happening exactly during the 900 s period, which could lead to an inaccurate indication of the power requirements and energy throughput of the storage devices for more volatile loads. Additionally, no conclusions can be drawn from this new data set about actual ramp rates. In summary, the flexibility

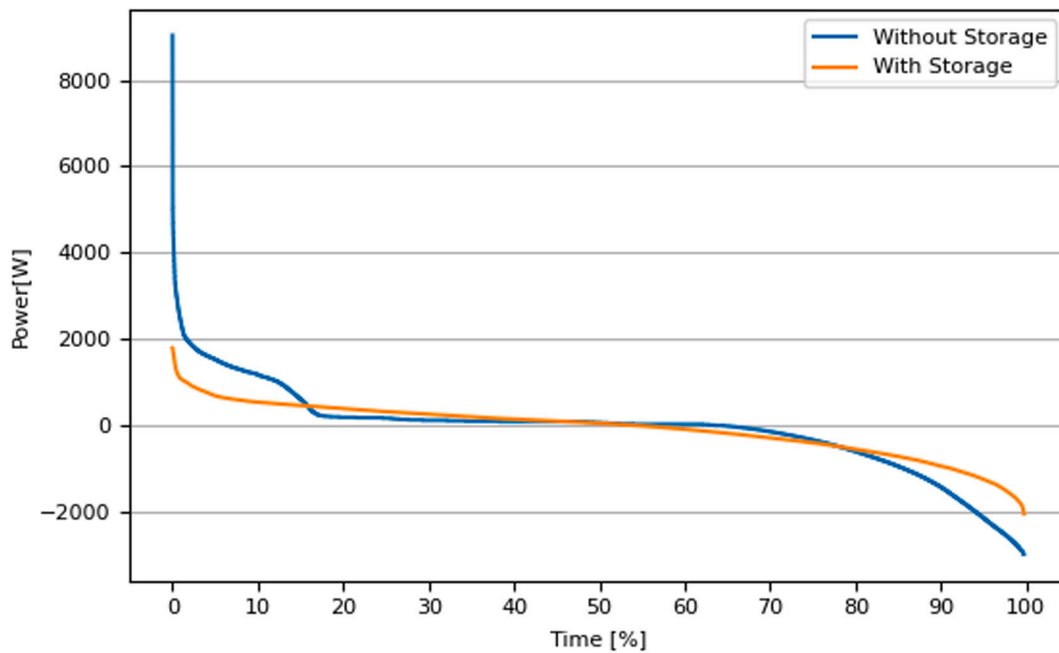


Fig. 15. Original and improved load duration curve, one year.

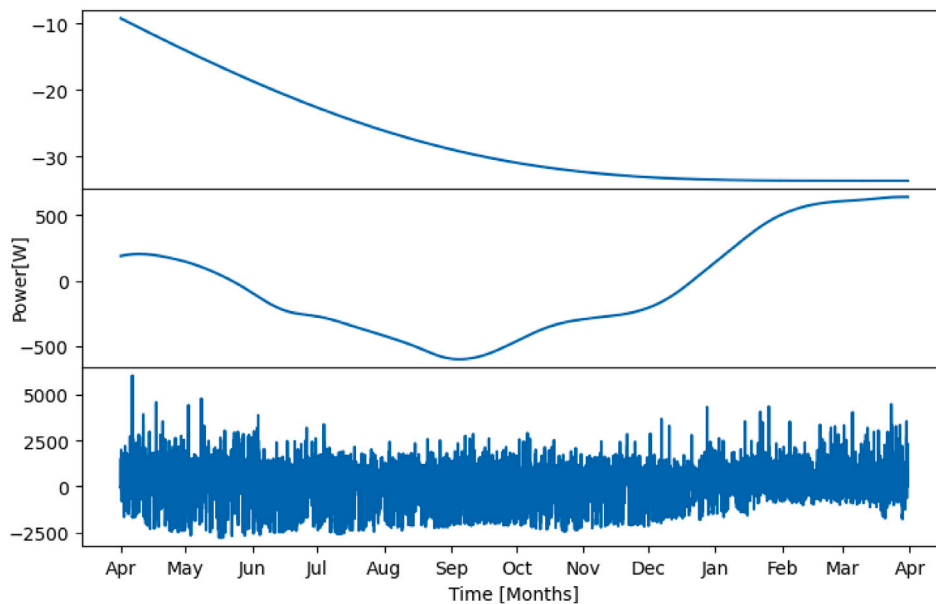


Fig. 16. Sub-profiles, 15 min down-sampled data, P^{dy} (top), P^{hr} (middle) and P^{rs} (bottom).

characteristics of the imbalance, and therefore the requirements on storage devices, becomes less evident.

It is not possible to derive one or more storage solutions from the sub-profiles created using the 900 s load data using the proposed method on a time-scales lower than 30 min due to having to adhere to the Nyquist frequency constraint. The P_{mn} profile was not created and a cut-off of one hour was still adhered to, in order to keep in line with the baseline storage technology time-scales discussed earlier. As detailed in Section 2, storage devices work best at time-scales specific to that technology. If an attempt was made in to link the sub-profiles to storage technologies, it is likely that a number of possible flexibility requirements derived from the sub-profiles would not be suitable for consideration. However, with more granular data more accurate and considerable flexibility requirements may become possible. This is an argument for using data granularity that is suitable for the use case

being examined. In the case of a household, the lower time-scales are relevant, and should be accounted for.

4.6. Benchmark testing

This section investigates the computational time of the tool that was created in Python in order to test the proposed method for several data set sizes. This tool is divided into two parts. Part I reads the original load profile, filters and splits the load profile into sub-profiles. These sub-profiles are then written to .csv files. Part II reads the individual sub-profiles and gathers the power, ramp-rate and capacity data per sub-profile, as well as creates the improved profile. This meta-data is written to .csv files.

Testing is conducted on a Intel core i7-7500U CPU @2.70 GHz. This is carried out for different sample sizes of data, with 10 s sample

Table 7
Benchmark testing.

Sample size	Part I (s)	Part II (s)
100k	2.03	1.64
200k	3.07	2.70
500k	6.05	5.90
1000k	10.92	12.22
3000k	30.96	33.53

frequency data being used as input and creating four sub-profiles. Table 7 shows the achieved results for the 10 s data set.

The computational time for an entire demonstration of the methodology for approximately one year of 10 s data (just over 3000 k samples) is just over one minute. This tool allows for a quick preliminary acquisition of requirements for multiple storage devices, based on large amounts of input data. The proposed method is therefore best suited for data sets over long periods with high granularity.

5. Conclusions and future work

To summarize, an approach has been presented to create sub-profiles from a given overall profile using a frequency filtering methodology. This approach is considered to be used as a preliminary investigation methodology that focuses on splitting based on frequency and creating a corresponding sizing but does not account for specific storage technologies. In a first step, a given number of sub-profiles are created using low-pass filters with cut-off frequencies which are chosen based on time-scale categories inherent to storage technologies. Based on these sub-profiles an estimate is made of storage capacity, power and ramp rate requirements, using a rudimentary storage model. Note, that this step can be augmented with a more in depth analysis of the load profile data using heat maps, in order to ascertain flexibility requirements for multiple frequencies. The basic aim of the methodology is to provide an easy and fast way to give insights into the necessary storage flexibility for a given situation. Furthermore, it is specifically suitable for high granularity data sets over longer periods of time. Additionally, for the investigated household use case, the method proves valuable for finding the requirements of a HESS which reduce the flexibility required from a grid connection to handle a power imbalance. The maximum power imported from the connected grid is reduced by approximately 7000 W the maximum power exported to the main grid is reduced by approximately 1000 W.

In future work, the proposed method should be tested with additional data sets, in order to ascertain how well the method performs for these data sets. Furthermore, methods for linking each sub-profile to a specific storage technology based on given specifications of these technologies may be integrated. Here, also financial indicators could play a role, as well as other technical indicators which may be added as constraints. In practice, a group of storage solutions could be derived to increase flexibility for a use case, with the storage devices chosen from a pool of possible technologies. Heat maps used also in an overall approach could be a useful tool here, and integrated into the larger methodology. Additionally, it would be interesting to investigate how the proposed method would perform when analysing a single load profile input, for example a household, compared to analysing a combination of load profile inputs, for example a neighbourhood. Finally, the influence of data sensitive to seasons of the year (such as wind or PV generation, or demand profiles with heat pumps or air conditioning) should be investigated in relation to the accuracy of defining the required flexibility of energy storage based on the amount of data available.

CRediT authorship contribution statement

E.W. Schaefer: Conceptualization, Methodology, Software, Validation, Formal analysis, Investigation, Resources, Data curation, Writing—original draft, Writing – review and editing, Visualization, Project administration. **G. Hoogsteen:** Conceptualization, Methodology, Formal analysis, Writing – review and editing, Supervision. **J.L. Hurink:** Writing – review and editing, Supervision, Project administration, Funding acquisition. **R.P. van Leeuwen:** Writing – review and editing, Supervision, Project administration, Funding acquisition.

Declaration of competing interest

The authors declare that they have no known competing financial interests or personal relationships that could have appeared to influence the work reported in this paper.

Acknowledgment

All authors have read and agreed to the published version of the manuscript. Research is part of European Regional Development Fund PROJ-00939.

References

- [1] E. Hsieh, R. Anderson, Grid flexibility: The quiet revolution, *Electr. J.* 30 (2) (2017) 1–8, <http://dx.doi.org/10.1016/j.tej.2017.01.009>.
- [2] D. Mohler, D. Sowder, Chapter 23 - Energy storage and the need for flexibility on the grid, in: L.E. Jones (Ed.), *Renewable Energy Integration*, Academic Press, Boston, 2014, pp. 285–292, <http://dx.doi.org/10.1016/B978-0-12-407910-6.00023-5>.
- [3] S. Aggarwal, R. Orvis, *Grid Flexibility: Methods for Modernizing the Power Grid*, Tech. rep., Energy Innovation, 2016.
- [4] S. Hajiaghahi, A. Salemnia, M. Hamzeh, Hybrid energy storage system for microgrids applications: A review, *J. Energy Storage* 21 (2019) 543–570, <http://dx.doi.org/10.1016/j.est.2018.12.017>.
- [5] S. Günther, A. Bensmann, R. Hanke-Rauschenbach, Theoretical dimensioning and sizing limits of hybrid energy storage systems, *Appl. Energy* 210 (2018) 127–137, <http://dx.doi.org/10.1016/j.apenergy.2017.10.116>.
- [6] S. Koohi-Fayegh, M. Rosen, A review of energy storage types, applications and recent developments, *J. Energy Storage* 27 (2020) 101047, <http://dx.doi.org/10.1016/j.est.2019.101047>.
- [7] E. Hossain, H.M.R. Faruque, M.S.H. Sunny, N. Mohammad, N. Nawar, A comprehensive review on energy storage systems: Types, comparison, current scenario, applications, barriers, and potential solutions, policies, and future prospects, *Energies* 13 (14) (2020) <http://dx.doi.org/10.3390/en13143651>.
- [8] S. Sabihuddin, A.E. Kiprakis, M. Mueller, A numerical and graphical review of energy storage technologies, *Energies* 8 (1) (2015) 172–216, <http://dx.doi.org/10.3390/en8010172>.
- [9] O. Krishan, S. Suhag, An updated review of energy storage systems: Classification and applications in distributed generation power systems incorporating renewable energy resources, *Int. J. Energy Res.* 43 (12) (2019) 6171–6210, <http://dx.doi.org/10.1002/er.4285>.
- [10] F. Nadeem, S.M.S. Hussain, P.K. Tiwari, A.K. Goswami, T.S. Ustun, Comparative review of energy storage systems, their roles, and impacts on future power systems, *IEEE Access* 7 (2019) 4555–4585, <http://dx.doi.org/10.1109/ACCESS.2018.2888497>.
- [11] X. Luo, J. Wang, M. Dooner, J. Clarke, Overview of current development in electrical energy storage technologies and the application potential in power system operation, *Appl. Energy* 137 (2015) 511–536, <http://dx.doi.org/10.1016/j.apenergy.2014.09.081>.
- [12] H. Ibrahim, A. Ilinca, J. Perron, Energy storage systems—Characteristics and comparisons, *Renew. Sustain. Energy Rev.* 12 (5) (2008) 1221–1250, <http://dx.doi.org/10.1016/j.rser.2007.01.023>.
- [13] H. SedighNejad, T. Iqbal, J. Quaicoe, Compressed air energy storage system control and performance assessment using energy harvested index, *Electronics* 3 (1) (2014) 1–21, <http://dx.doi.org/10.3390/electronics3010001>.
- [14] P. Denholm, T. Mai, Timescales of energy storage needed for reducing renewable energy curtailment, *Renew. Energy* 130 (2019) 388–399, <http://dx.doi.org/10.1016/j.renene.2018.06.079>.
- [15] Y. Yang, S. Bremner, C. Menictas, M. Kay, Battery energy storage system size determination in renewable energy systems: A review, *Renew. Sustain. Energy Rev.* 91 (2018) 109–125, <http://dx.doi.org/10.1016/j.rser.2018.03.047>.
- [16] Quintel, Loss of load expectation: Energy transition model, 2021, URL <http://docs.energytransitionmodel.com/main/loss-of-load-expectation/>.

- [17] S. Hajiaghahi, A. Salemnia, M. Hamzeh, Hybrid energy storage system for microgrids applications: A review, *J. Energy Storage* 21 (2019) 543–570, <http://dx.doi.org/10.1016/j.est.2018.12.017>.
- [18] I. San Martín, A. Ursúa, P. Sanchis, Integration of fuel cells and supercapacitors in electrical microgrids: Analysis, modelling and experimental validation, *Int. J. Hydrogen Energy* 38 (27) (2013) 11655–11671, <http://dx.doi.org/10.1016/j.ijhydene.2013.06.098>.
- [19] G. Wang, M. Ciobotaru, V.G. Agelidis, Optimal capacity design for hybrid energy storage system supporting dispatch of large-scale photovoltaic power plant, *J. Energy Storage* 3 (2015) 25–35, <http://dx.doi.org/10.1016/j.est.2015.08.006>.
- [20] H. Jia, Y. Mu, Y. Qi, A statistical model to determine the capacity of battery–supercapacitor hybrid energy storage system in autonomous microgrid, *Int. J. Electr. Power Energy Syst.* 54 (2014) 516–524, <http://dx.doi.org/10.1016/j.ijepes.2013.07.025>.
- [21] A. Abbassi, M.A. Dami, M. Jemli, A statistical approach for hybrid energy storage system sizing based on capacity distributions in an autonomous PV/Wind power generation system, *Renew. Energy* 103 (2017) 81–93, <http://dx.doi.org/10.1016/j.renene.2016.11.024>.
- [22] Y. Ghiassi-Farrokhfal, C. Rosenberg, S. Keshav, M.-B. Adjaho, Joint optimal design and operation of hybrid energy storage systems, *IEEE J. Sel. Areas Commun.* 34 (3) (2016) 639–650, <http://dx.doi.org/10.1109/JSAC.2016.2525599>.
- [23] H. Chen, Z. Zhang, C. Guan, H. Gao, Optimization of sizing and frequency control in battery/supercapacitor hybrid energy storage system for fuel cell ship, *Energy* 197 (2020) 117285, <http://dx.doi.org/10.1016/j.energy.2020.117285>.
- [24] M. Masih-Tehrani, M.-R. Ha'iri-Yazdi, V. Esfahanian, A. Safaei, Optimum sizing and optimum energy management of a hybrid energy storage system for lithium battery life improvement, *J. Power Sources* 244 (2013) 2–10, <http://dx.doi.org/10.1016/j.jpowsour.2013.04.154>, 16th International Meeting on Lithium Batteries (IMLB).
- [25] Y. Zhang, X. Tang, Z. Qi, Z. Liu, The Ragone plots guided sizing of hybrid storage system for taming the wind power, *Int. J. Electr. Power Energy Syst.* 65 (2015) 246–253, <http://dx.doi.org/10.1016/j.ijepes.2014.10.006>.
- [26] I. Janghorban Esfahani, S. Lee, C. Yoo, Extended-power pinch analysis (EPoPA) for integration of renewable energy systems with battery/hydrogen storages, *Renew. Energy* 80 (2015) 1–14, <http://dx.doi.org/10.1016/j.renene.2015.01.040>.
- [27] A.S. Jacob, R. Banerjee, P.C. Ghosh, Sizing of hybrid energy storage system for a PV based microgrid through design space approach, *Appl. Energy* 212 (2018) 640–653, <http://dx.doi.org/10.1016/j.apenergy.2017.12.040>.
- [28] P. Zhao, J. Wang, Y. Dai, Capacity allocation of a hybrid energy storage system for power system peak shaving at high wind power penetration level, *Renew. Energy* 75 (2015) 541–549, <http://dx.doi.org/10.1016/j.renene.2014.10.040>.
- [29] S. Wen, H. Lan, D.C. Yu, Q. Fu, Y.-Y. Hong, L. Yu, R. Yang, Optimal sizing of hybrid energy storage sub-systems in PV/diesel ship power system using frequency analysis, *Energy* 140 (2017) 198–208, <http://dx.doi.org/10.1016/j.energy.2017.08.065>.
- [30] Y. Liu, W. Du, L. Xiao, H. Wang, S. Bu, J. Cao, Sizing a hybrid energy storage system for maintaining power balance of an isolated system with high penetration of wind generation, *IEEE Trans. Power Syst.* 31 (4) (2016) 3267–3275, <http://dx.doi.org/10.1109/TPWRS.2015.2482983>.
- [31] L. Lévesque, Nyquist sampling theorem: understanding the illusion of a spinning wheel captured with a video camera, *Phys. Educ.* 49 (6) (2014) 697–705, <http://dx.doi.org/10.1088/0031-9120/49/6/697>.
- [32] A.R. Hambley, *Electrical Engineering Principles and Applications*, sixth ed., Pearson Education Inc., New Jersey, 2014, pp. 278–332.
- [33] M. Dotzauer, D. Pfeiffer, M. Lauer, M. Pohl, E. Mauky, K. Bär, M. Sonnleitner, W. Zörner, J. Hudde, B. Schwarz, B. Faßauer, M. Dahmen, C. Rieke, J. Herbert, D. Thrän, How to measure flexibility – Performance indicators for demand driven power generation from biogas plants, *Renew. Energy* 134 (2019) 135–146, <http://dx.doi.org/10.1016/j.renene.2018.10.021>.
- [34] E. Corsetti, S. Riaz, M. RIELLO, P. Mancarella, Modelling and deploying multi-energy flexibility: The energy lattice framework, *Adv. Appl. Energy* 2 (2021) 100030, <http://dx.doi.org/10.1016/j.adapen.2021.100030>.
- [35] A. Ulbig, G. Andersson, Chapter 18 - Role of power system flexibility, in: L.E. Jones (Ed.), *Renewable Energy Integration*, Academic Press, Boston, 2014, pp. 227–238, <http://dx.doi.org/10.1016/B978-0-12-407910-6.00018-1>.
- [36] Saxion University of Applied Sciences, University of Twente, Load Profile Analysis Tool (LPAT), 2021, URL <https://github.com/edmundschaefer84/LPAT.git>.